10582 *Biochemistry* **2010,** *49,* 10582–10588
DOI: 10.1021/bi101542t

BIOCHEMISTRY
including biophysical chemistry & molecular biology
Article

The Second-Shell Metal Ligands of Human Arginase Affect Coordination of the Nucleophile and Substrate[†]

Everett M. Stone,[‡] Lynne Chantranupong,[‡] and George Georgiou*[,‡,§]

[‡]*Departments of Chemical Engineering and Biomedical Engineering and* [§]*Department of Molecular Genetics and Microbiology and Institute for Molecular and Cell Biology, University of Texas, Austin, Texas 78712, United States*

Received September 22, 2010; Revised Manuscript Received November 4, 2010

ABSTRACT: The active sites of eukaryotic arginase enzymes are strictly conserved, especially the first- and second-shell ligands that coordinate the two divalent metal cations that generate a hydroxide molecule for nucleophilic attack on the guanidinium carbon of L-arginine and the subsequent production of urea and L-ornithine. Here by using comprehensive pairwise saturation mutagenesis of the first- and second-shell metal ligands in human arginase I, we demonstrate that several metal binding ligands are actually quite tolerant to amino acid substitutions. Of >2800 double mutants of first- and second-shell residues analyzed, we found more than 80 unique amino acid substitutions, of which four were in first-shell residues. Remarkably, certain second-shell mutations could modulate the binding of both the nucleophilic water/hydroxide molecule and substrate or product ligands, resulting in activity greater than that of the wild-type enzyme. The data presented here constitute the first comprehensive saturation mutagenesis analysis of a metallohydrolase active site and reveal that the strict conservation of the second-shell metal binding residues in eukaryotic arginases does not reflect kinetic optimization of the enzyme during the course of evolution.

Arginases (EC 3.5.3.1) are typically homotrimeric enzymes with an α/β fold comprising an eight-strand β-sheet surrounded by several helices. The enzyme contains a dinuclear metal center that generates a hydroxide for nucleophilic attack on the guanidinium carbon of L-arginine (L-Arg)[1] (*1*, *2*). The structure of arginase shows an active site cleft containing two divalent metal ions (M_A and M_B) (Figure 1), with the more deeply localized ion designated M_A coordinated to first-shell ligands H101, D124, D128, and D232 (human arginase I numbering) and a bridging hydroxide. The other metal is designated M_B and is coordinated by first-shell ligands H126, D124, D232, and D234 and a bridging hydroxide (*3*). The first-shell ligands are strictly conserved among all arginases. The second-shell ligands, defined as those residues that contribute a hydrogen bond to the first-shell ligands, are important in stabilizing and orienting the metal-binding first-shell ligands. The second-shell ligands are comprised of W122, D181, and S230 (Figure 1), which form hydrogen bonds through their side chains to first-shell ligands D124, H126, and H101, respectively.

The native metal for arginases has long been thought to be manganese, although some arginases from bacteria such as *Helicobacter pylori* and *Bacillus anthracis* are likely to incorporate cobalt and nickel, respectively, under physiological conditions (*4*, *5*). We recently reported that incorporation of cobalt in human arginase I (hArgI) results in much greater activity (k_{cat}/K_M) at the serum pH (7.4) (*6*). In serum, cobalt-substituted human arginase I (Co-hArgI) displays a >10-fold lower K_M for L-Arg and approximately 5-fold greater stability relative to that of the manganese enzyme (Mn-hArgI). Co-hArgI is currently being investigated as an antineoplastic agent for the depletion of serum L-Arg, which induces apoptosis of L-Arg auxotrophic tumors.

There is relatively little information about the effects of amino acid substitutions in the first- and second-shell residues in arginases, with the exception of some single site-directed mutations (*1*, *7*−*9*). Phylogenetic analysis of arginases reveals that the first-shell ligands are strictly conserved from bacteria to humans. The second-shell ligands are strictly conserved in eukaryotes and are found to vary slightly in only a few arginases of bacterial origin such as *H. pylori* and *Bacillus* species.

In this study, we sought (i) to examine whether the striking conservation of the metal binding sites in arginase reflects catalytic optimization of the enzyme during evolution, i.e., in other words whether amino acid substitutions in first- or second-shell residues uniformly result in reduced activity, (ii) to evaluate the amino acid plasticity of the metal binding site, and (iii) to compare whether first- and second-shell mutations might exert a differential effect on activity with Co^{2+} relative to Mn^{2+}. Finally, (iv) we sought to identify amino acid substitutions in the metal binding ligands that improve the pharmacological efficacy of Co-hArgI. First- and second-shell ligand residues were subjected to pairwise combinatorial saturation mutagenesis followed by semi-quantitative rank ordering of active enzyme variants and detailed kinetic analyses. Analysis of >2800 Co-hArgI variants revealed a sizable number of amino acid substitutions in second-shell residues that confer appreciable catalytic activity at physiological pH, a few even resulting in a higher k_{cat}/K_m relative to that of the parental enzyme. For these mutants, higher catalytic activity was observed with both Co^{2+} and Mn^{2+}.

[†]This project was funded by Grant HF0032 from TI3D/Welch Foundation and National Institutes of Health Grant CA 139059. L.C. was supported by a fellowship from the Arnold and Mabel Beckman Foundation.

*To whom correspondence should be addressed: 1 University Station, C0800 Austin, TX 78712-1084. Phone: (512) 471-6975. Fax: (512) 471-7963. E-mail: gg@che.utexas.edu.

[1]Abbreviations: wt, wild type; L-Arg, L-arginine; M_A and M_B, metal ions A and B, respectively; hArgI, human arginase I; IPTG, isopropyl β-D-1-thiogalactopyranoside; IMAC, immobilized metal affinity chromatography; MWCO, molecular weight cutoff.

 Published on Web 11/05/2010

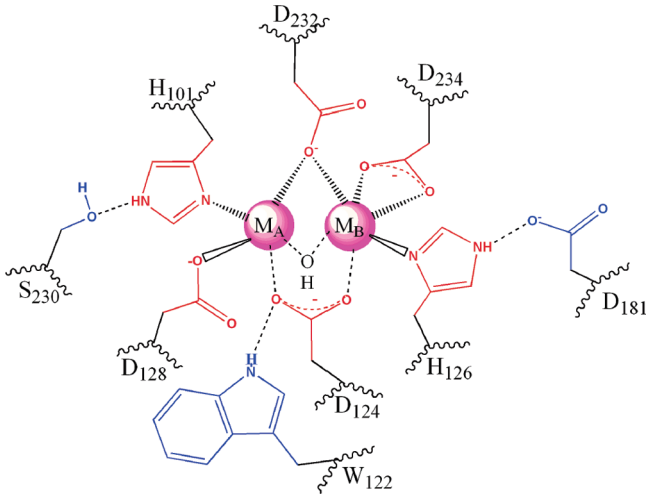

FIGURE 1: Depiction of the active site of hArgI with first-shell metal ligands (red) and second-shell ligands (blue) coordinating two metal cations necessary for activity.

These results suggest that (a) fine-tuning of the metal ligands can be employed to enhance catalytic activity under certain conditions, (b) the Co-hArgI variants displaying improved catalytic properties under physiological conditions are likely to be useful for therapeutic purposes, and (c) the high degree of conservation and the elevated pH optimum of arginases do not reflect evolutionary selection for catalytic activity and therefore are likely to have arisen in response to more subtle selective pressures. (d) Changes in the second-shell ligand coordinating H101 modulate the Lewis acidity of M_A.

EXPERIMENTAL PROCEDURES

General Cloning. Genes of hArgI variants containing an N-terminal six-His tag were cloned into pET28a plasmids for sequence and expression as described previously (*6*).

Development of a 96-Well Plate Screen. Single colonies of *Escherichia coli* BL21-containing plasmids encoding either wild-type (control) or variant arginase enzymes were picked into 96-well culture plates containing 75 μL of TB medium/well and 50 μg/mL kanamycin. Cells were grown at 37 °C on a plate shaker to an OD_{600} of ~0.8−1 and cooled to 25 °C, whereupon an additional 75 μL of medium containing 50 μg/mL kanamycin and 0.5 mM IPTG were added, and incubation with shaking was continued for 2 h at 25 °C. Subsequently, 100 μL of culture/well was transferred to a fresh 96-well plate (assay plate). The assay plates were centrifuged (10 min at 3500*g*) to pellet the cells; the medium was removed, and the cells were chemically lysed by addition of 50 μL of B-PER protein extraction reagent per well (Pierce, Rockford, IL) and mixing for 5 min on a plate shaker. An additional 50 μL of 200 μM L-Arg, 10 μM $CoCl_2$, in 100 mM HEPES buffer (pH 7.4) per well were subsequently added, and reactions were allowed to proceed for 1−5 min at 25 °C. Reactions were quenched with 100 μL of color developing reagent per well, and plates were incubated at 95 °C for 15 min, as described previously (*10*). Lysates from colonies having the ability to produce urea produced a bright red dye with a λ_{max} of 530 nm.

High-Throughput Purification and Kinetic Screening of Variants. A small-scale purification scheme was developed to rapidly purify dozens of proteins at once for kinetic analysis. Cultures (50 mL) of *E. coli* expressing arginase were grown in 125 mL shake flasks and induced for protein synthesis and harvested as described previously (*6*). Aliquots (5 mL) were centrifuged, and the resulting cell pellets were lysed with 400 μL of B-PER protein extraction reagent (Pierce) (50 mL scale cultures had better expression levels, and the remaining 45 mL of culture pellets was frozen for later use). The soluble fractions were then mixed with 500 μL of IMAC lysis buffer and 100 μL of IMAC beads (Talon, Mountain View, CA) in a 1.5 mL Eppendorf tube. After a 2 min incubation, the suspensions were centrifuged at 3000 rpm for 20 s in a tabletop centrifuge. The supernatants were discarded; arginase-bound beads were washed with 2 × 1 mL of IMAC lysis buffer by mixing and centrifugation, and the supernatant was discarded. Arginase was then eluted from the beads by addition of 300 μL of IMAC elution buffer followed by another centrifugation step. The resulting arginase-containing supernatants were buffer exchanged twice with 100 mM Hepes buffer (pH 7.4) using a 10000 MWCO centrifugal concentration device (YM-10 Amicon). The protein was quantified by measuring A_{280} and heat incubated with 100 μM $CoCl_2$, and purity was assessed by sodium dodecyl sulfate−polyacrylamide gel electrophoresis (SDS−PAGE). This method allows purification of 12−16 proteins in ~2 h with a yield of 200−300 μg of protein with the purity varying between 60 and 95% as assessed by SDS−PAGE.

The rate of L-Arg hydrolysis was evaluated by incubating 24 nM purified enzyme with 200 μM L-Arg in microtiter plate wells. Aliquots were taken at different time points, and the reaction was immediately quenched when the sample was mixed with the acidic color-developing reagent in separate 96-well plates (*10*). Progress curve data were fit to an exponential eq 1

$$y = y_{max}[1 - e^{-(V/K)[E]t}] \quad (1)$$

where y is the absorbance at 530 nm, y_{max} is the asymptote, t is the time, [E] is the enzyme concentration, and V/K is the apparent specificity constant. This method allows the rank ordering of four enzyme variants per 96-well plate in triplicate in ~30 min.

Engineering the First- and Second-Shell Metal Ligands of Arginase for Optimal Activity. The following saturation libraries at first- and second-shell metal ligand positions were constructed: H101 and S230 (library 1), H126 and D181 (library 2), D124 and W122 (library 3), two first-shell residues D124 and D232 (library 4), and two second-shell positions D181 and S230 (library 5). The first-shell positions were randomized with a NRS codon scheme in which N is A, C, T, or G, R is A or G, and S is G or C: the second-shell positions were randomized using an NNS codon scheme (the oligonucleotides for library construction are summarized in the Supporting Information). Following digestion with NcoI and BamHI, the library DNA was ligated into pET28a, the ligation mixtures were transformed into *E. coli* BL21, and transformants were screened as described above. Clones displaying activity were identified by sequencing, retransformed into *E. coli* BL21, purified (small scale), and kinetically characterized via determination of progress curves as described above. Variants displaying an apparent V/K equal to or greater than that of the wild type were purified on a larger scale (50 mL of culture) and assayed for their steady-state kinetic parameters (k_{cat} and K_M).

Expression and Purification of hArgI Variants. hArgI variants were expressed, purified, and loaded with either Co^{2+} or Mn^{2+} as described previously (*6*).

pH Rate Dependence of Arginase Variants. The pH rate dependence of cobalt-substituted S230C, S230G, D181N, and S230G/D181N and manganese-substituted S230G/D181N

Scheme 1: High-Throughput Screening and Analysis[a]

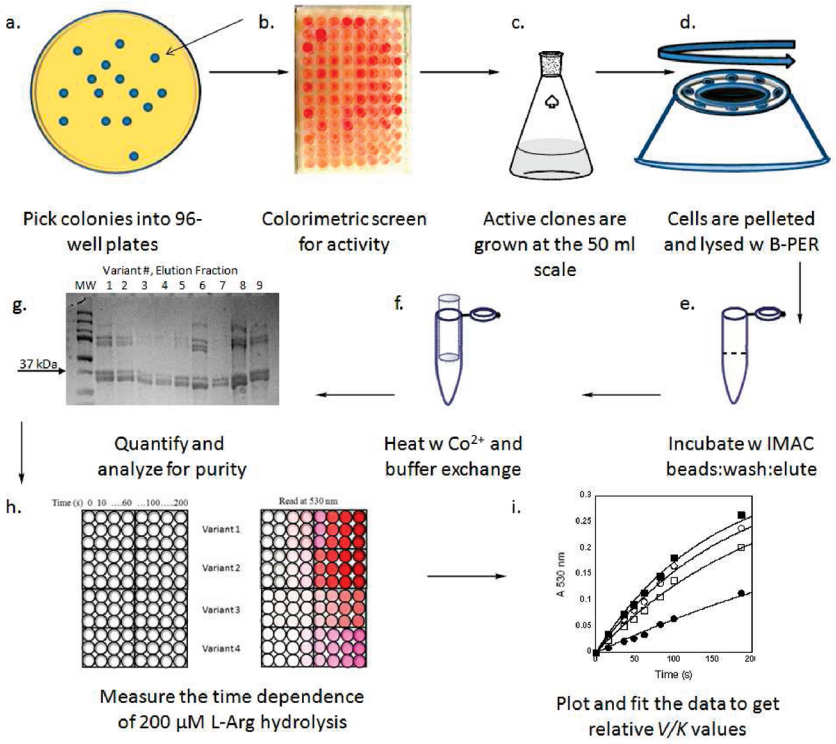

[a](a) Colonies harboring plasmids containing mutagenized hArgI fused to an N-terminally encoded His_6 tag are picked into 96-well culture plates for expression. (b) Microtiter scale cultures are lysed and screened for activity. (c) Active clones are grown at the 50 mL scale. (d) Cells are pelleted and lysed with B-PER. (e) Soluble fractions are incubated with IMAC beads followed by elution. (f) After being heat incubated with Co^{2+}, the resulting protein is buffer exchanged using a centrifugal device. (g) A SDS−PAGE gel is run to assess protein yield and purity. (h) The rate of hydrolysis of L-Arg is measured in triplicate in 96-well plates. (i) The data are plotted and fit to obtain apparent V/K values.

arginase variants was determined by measuring the steady-state rate constants across a broad range of pH values at 37 °C. The following buffers were used: sodium acetate at pH 5−5.5, MES at pH 6−6.5, HEPES at pH 7−7.8, Tris at pH 8−9, and Capso at pH 9−10.5, all at concentrations of 100 mM. The ionic strength of these buffers at varying pH values ranged from 0.011 to 0.087 M. All enzyme reactions were performed in at least triplicate at 37 °C. Mn^{2+}- or Co^{2+}-substituted hArgI variants were each assayed with a range of substrate concentrations from 30 μM to 80 mM, depending on the pH. After the kinetic data had been fit to the Michaelis−Menten equation, the k_{cat} and k_{cat}/K_M values were calculated and plotted versus pH. The resulting data were fit to a form of the Henderson−Hasselbalch equation, as described previously (*6*). The k_{cat}/K_M values of all enzymes exhibited a bell-shaped curve with two apparent pK_a values closer than 3 pH units, and thus, Segel's method was used to correct the fitted pK_a values (*11*). The pH dependence of k_{cat} was also fit to a one-pK_a model for Mn-hArgI-S230G/D181N.

Product Inhibition Kinetics. Co-hArgI-D181N, Co-hArgI-S230G, Co-hArgI-S230C, or Co-hArgI-D181N/S230G was incubated with 0.3, 0.2, 0.15, or 0.3 mM L-Arg, respectively, in 100 mM HEPES buffer (pH 7.4) at 37 °C with varying concentrations of L-ornithine (L-Orn) up to 1 mM. Mn-hArgI-D181N, Mn-hArgI-D181N/S230G, or Mn-hArgI-S230G was incubated with 1 mM L-Arg and varying concentrations of L-Orn (0−10 mM). Data were expressed as percent activity, plotted versus L-Orn concentration, and fit to an exponential equation to determine IC_{50} values. The K_i values were calculated using eq 2, assuming a competitive mechanism and using K_M values determined under identical conditions.

$$K_i = \frac{IC_{50}}{1 + \frac{[S]}{K_M}} \quad (2)$$

RESULTS

Scanning Saturation Mutagenesis of First- and Second-Shell Metal Ligands. We performed pairwise combinatorial saturation mutagenesis to explore the role of first- and second-shell metal ligand amino acids in Co-hArgI (Figure 1). We constructed five pairwise saturation libraries at the following first- and second-shell positions: H101 and S230 (library 1), H126 and D181 (library 2), D124 and W122 (library 3), D124 and D232 (both first-shell residues, library 4), and D181 and S230 (both second-shell residues, library 5). To analyze the activity of the respective enzyme variants, we developed a high-throughput semiquantitative assay system, as follows (Scheme 1). First, a colorimetric 96-well plate assay was developed to monitor the formation of urea by hArgI. The assay was shown to have a dynamic range of ~5−300 μM for the ureido product (*6*). We used $CoCl_2$ and low L-Arg concentrations to screen for activity because of the high k_{cat}/K_M values we had previously observed, but the screen can be adapted for use with any suitable divalent metal. Second, we devised a rapid semiquantitative expression and purification method that allows the production of 16 enzyme variants in ~2 h with a yield of 200−300 μg of protein at 60−90% purity as assessed by SDS−PAGE. Third, progress curves in a 96-well plate format

were employed to determine apparent k_{cat}/K_M values. In general, most hArgI variants were solubly expressed at near-wt levels, making this a convenient assay method for rank ordering selected enzymes.

Libraries were created by mutagenizing the desired pairs of codons by using either an NRS (R is A or G, and S is G or C) and/or NNS randomization. At least 1000−2000 clones from each library (> 2-fold coverage vs the theoretical codon diversity) were analyzed, for ~6000 clones in total. Active enzyme variants were rank ordered relative to wt Co-hArgI activity and sequenced to determine the respective mutations. The percentage of active clones from each library varied greatly. Library 1 (H101 and S230) had ~6% active clones. H101 was largely conserved, and we found only two double mutants: H101N/S230C and H101D/S230H (Table S1 of the Supporting Information). Library 2 (H126 and D181) had 8% active clones, and we also found only two double mutants, H126N/D181Q and H126Q/D181A, with the rest of the mutations occurring only at the D181 position (Table S2 of the Supporting Information). Library 3 (D124 and W122) had 3% active clones with D124 being strictly conserved (Table S3 of the Supporting Information). Library 4 (D124 and D232) had 2% active clones, which turned out to encode synonymous codons that gave rise to the wt enzyme. Library 5 (D181 and S230) had 18% active clones with a broad variety of single and double mutations (Table S4 of the Supporting Information).

Collectively, the data from the combinatorial saturation mutagenesis of the hArgI metal ligand residues show that the first shell is highly conserved, with only H101 and H126 tolerating substitutions with Asp, Asn, or Gln, along with a corresponding second-shell mutation. However, all the first-shell ligand mutations resulted in a significant loss of L-Arg hydrolysis catalytic activity. In contrast, the second-shell ligands exhibited a much higher degree of plasticity. For example, 16 of 19 substitutions in D181 resulted in enzymes having appreciable activity, with 13 substitutions yielding > 40% of the activity of the wt enzyme. In general, the substitutions that gave the highest apparent rates resulted from residues that are able to form a hydrogen bond (i.e., Ser, Thr, and Asn) or residues that might allow a water molecule to form a hydrogen bond with the imidazole proton of H126 (i.e., Ala and Gly). Apparent, second-order L-Arg hydrolysis rates were significantly decreased in enzymes containing amino acid substitutions with large hydrophobic residues (Tyr and Trp) or positively charged residue Arg or Lys.

The library of D124 and W122 showed absolute conservation of the first-shell D124 residue, and only a few amino acids were observed to substitute for W122, resulting in greatly reduced activity (Table S3 of the Supporting Information). It is interesting to note that alignments of arginase from *H. pylori* show a Tyr residue at this position. An interruption of the hydrogen bond from the indole nitrogen to D124 may be a reason why the catalytic rate of *H. pylori* arginase is several orders of magnitude slower than those of most arginases (*5*).

The second-shell ligand to H101, S230, resides in the interior of the enzyme. Therefore, not surprisingly, very large substitutions were excluded from this site. The enzyme variants that gave the highest apparent second-order rates were again mutations to amino acids capable of forming a hydrogen bond or allowing a water molecule access to this site (i.e., Cys, Thr, and Gly). Lower apparent V/K values were observed with the addition of a negative charge (Asp) or with hydrophobic residues (i.e., Met and Val).

When the two second-shell ligands, D181 and S230, were subjected to pairwise saturation mutagenesis, a large number of unique mutants displaying a significant amount of activity were found. In general, the trends in the amino acid substitutions allowed were the same as with the single second-shell ligand variants, with the highest apparent activity seen when the wt amino acids were replaced with residues that can accept a hydrogen bond or allow access to a water molecule. In particular, most of the active enzyme variants from this library had an either Gly, Thr, or Ala substitution at position 230.

Table 1: Steady-State Kinetic Characterization of Select hArgI Variants[a]

amino acid replacing D181	amino acid replacing S230	k_{cat} (s^{-1})	K_M (mM)	k_{cat}/K_M (s^{-1} mM^{-1})
		Cobalt(II)		
−	Gly	200 ± 7	0.08 ± 0.01	2600 ± 420[d]
−	Cys	327 ± 12	0.15 ± 0.02	2180 ± 360[d]
−	Thr	315 ± 13	0.16 ± 0.02	1970 ± 370
Glu	Ala	220 ± 7	0.15 ± 0.02	1470 ± 210
Ser	−	388 ± 13	0.28 ± 0.03	1390 ± 190
Asn	−	387 ± 17	0.30 ± 0.04	1290 ± 230
Glu	−	344 ± 8	0.27 ± 0.02	1270 ± 110
wt[b]	wt	240 ± 14	0.19 ± 0.04	1260 ± 330
Asn	Gly	247 ± 11	0.21 ± 0.03	1180 ± 220
Ser	Gly	180 ± 8	0.19 ± 0.03	950 ± 200
[c]	Asp	140 ± 3	0.15 ± 0.01	930 ± 80
		Manganese(II)		
−	Gly	266 ± 10	0.80 ± 0.1	330 ± 50[d]
Asn	Gly	517 ± 11	2.8 ± 0.2	185 ± 17[d]
−	Cys	285 ± 22	2.1 ± 0.4	136 ± 36
−[b] (wt)	− (wt)	300 ± 12	2.3 ± 0.3	130 ± 20
Asn	−	360 ± 24	3.0 ± 0.5	120 ± 15

[a]All enzymes were heat activated with Co^{2+} or Mn^{2+} as indicated. [b]From ref *6*. [c]Required excess Co^{2+} for measuring activity. [d]Significantly different from that of wt ($p < 0.05$).

Select variants displaying an apparent V/K of ≥80% compared to that of wt Co-hArgI were purified to greater than 95% homogeneity as determined by SDS−PAGE and loaded with either Co^{2+} or Mn^{2+}, and the resulting enzymes were analyzed in greater detail. Table 1 summarizes the Michaelis−Menten parameters at 37 °C and pH 7.4. The k_{cat}/K_M values of most of the variants analyzed were not significantly different from those of wt Co-hArgI ($p > 0.05$). However, the Co-hArgI-S230G and Co-hArgI-S230C variants exhibited significantly increased specificity constants. When Co^{2+} was replaced with Mn^{2+}, the S230G variant and the double mutant D181N/S230G also exhibited significant increases in k_{cat}/K_M. In particular, the Mn-hArgI-S230G variant exhibited a significantly reduced K_M for L-Arg (from 2.3 to 0.8 mM).

The effect of pH on the k_{cat}/K_M (and k_{cat} where applicable) values of several enzyme variants was also determined (Table 2). All the variants tested displayed a bell-shaped pH dependence curve similar to that of wt (*6*). The Co-hArgI-S230G mutant and the Co-hArgI-S230G/D181N double mutant had slightly depressed ascending limb pK_a values (pK_{a1}) compared to that of wt. An exception was Co-hArgI-S230C, which interestingly had a more narrow pH profile with an elevated pK_{a1} and a depressed pK_{a2} value (Figure S1 of the Supporting Information compares Co-hArgI-S230C and Co-hArgI-S230G). We also evaluated the pH dependence of k_{cat} and k_{cat}/K_M of the Mn-hArgI-D181N/S230G double mutant and found that ionizations in the free enzyme and free substrate (k_{cat}/K_M) were not drastically different from that of wt Mn-hArgI, but ionizations in the enzyme−substrate complex (k_{cat}) were depressed by 0.4 pH unit.

Table 2: pH Rate Dependence of Select hArgI Variants

	pK_{a1}	pK_{a2}
pH Dependence of k_{cat}		
Mn-hArgI[a]	8.1 ± 0.1	not applicable
Mn-hArgI-D181N/S230G	7.7 ± 0.1	not applicable
pH Dependence of k_{cat}/K_M		
Mn-hArgI[a]	8.5 ± 0.1	10.9 ± 0.2
Mn-hArgI-D181N/S230G	8.4 ± 0.1	9.9 ± 0.1
Co-hArgI-S230C	7.8 ± 0.1	9.0 ± 0.1
Co-hArgI[a]	7.5 ± 0.1	9.6 ± 0.1
Co-hArgI-D181N	7.4 ± 0.1	9.4 ± 0.1
Co-hArgI-S230G	7.0 ± 0.1	9.7 ± 0.1
Co-hArgI-D181N/S230G	7.0 ± 0.1	9.4 ± 0.1

[a]From ref *6*.

Table 3: Product Inhibition Constants of Select hArgI Variants

	K_I (mM) at pH 7.4
Mn-hArgI[a]	2.3 ± 0.1
Mn-hArgI-D181N	2.4 ± 0.2
Mn-hArgI-D181N/S230G	1.0 ± 0.25
Mn-hArgI-S230G	0.7 ± 0.1
Co-hArgI-D181N	0.11 ± 0.02
Co-hArgI-D181N/S230G	0.09 ± 0.02
Co-hArgI[a]	0.08 ± 0.02
Co-hArgI-S230G	0.05 ± 0.01

[a]From ref *6*.

Finally, product inhibition constants at 37 °C and pH 7.4 were determined for several variants (Table 3). We found that the S230G mutation not only lowers K_M but also results in the product binding more tightly. In contrast, the other second-shell mutation analyzed, D181N, does not show any appreciable difference in product binding compared to the wt enzyme.

DISCUSSION

The catalytic power of metallohydrolases stems in part from their remarkable ability to depress the pK_a of water (~16) to a much lower value and to coordinate the highly reactive hydroxide ion for attack on substrate. Both the kind of metal and its local environment, comprised of first- and second-shell ligands, can exert a dramatic effect on the catalytic rate, metal binding affinity, and pK_a of the nucleophilic water/hydroxide molecule (*3*). The effects of mutations on metal binding ligands have been explored more extensively in carbonic anhydrase (CA), a metallohydrolase for which a large amount of structural and mutational data has accumulated and biophysical characterization has been conducted. The active site of CA contains a Zn^{2+} molecule coordinated by three histidine ligands, His94, His96, and His119, and a solvent molecule. In turn, the protonated nitrogen atoms of the first-shell His ligands are hydrogen bonded to a second shell where the side chain of Gln92 is H-bonded to His94, the backbone carbonyl of Asn244 is H-bonded to His96, and the side chain of Glu117 is H-bonded to His119 (*12*). Fierke, Christianson, and others found that mutations of the first shell of CA generally led to large (~1000-fold) decreases in activity while mutations of the second-shell ligands to His94 and His119 resulted in moderately (3−10-fold) lower k_{cat}/K_M values but, depending on the

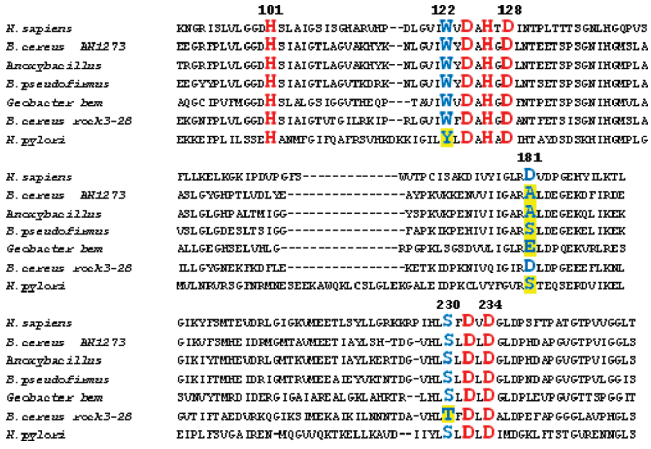

FIGURE 2: Sequence alignments of hArgI and arginases from several bacterial species showing the absolutely conserved first-shell ligand residues (red) and the highly conserved second-shell ligand residues (blue).

mutation, could modulate the pK_a of the zinc water/hydroxide nucleophile. To the best of our knowledge, no mutations in the first- or second-shell residues of CA or any other metallohydrolase that result in enhanced catalytic rates have been identified previously. In this work, we identified mutations of second-shell residue S230 of hArgI; namely, substitution with Gly, Cys, and, to a lesser extent, Thr results in significant rate enhancements at pH 7.4 for the Co^{2+}-containing enzyme. Similarly, Mn^{2+}-hArgI-S230G displayed a 2.5-fold higher k_{cat}/K_m at pH 7.4 relative to that of the parental enzyme.

Consistent with earlier reports, sequence alignments of eukaryotic arginases show a strict conservation in both the first- and second-shell ligands (*13*). The metal ligand sites of bacterial arginases are also highly conserved. We found only a few bacterial species in which a couple of second-shell residues, most notably D181 (human arginase numbering), were replaced instead with Ala, Ser, or Glu (Figure 2). This finding implies that the metal ligands in arginase enzymes may have undergone evolutionary optimization selecting for the optimal configuration that results in a maximal catalytic rate. Although we found two variants (S230G and S230C) with enhanced kinetics, they did not retain activity over time as well as wt, suggesting an evolutionary bias toward stability as well.

Earlier mutational studies of arginase reported that substitutions of first-shell residue D232 (with A or C) or D128 (with A, E, or N) drastically curtail enzymatic activity (*1*) whereas H101N and H126N variants retained 47−88% activity only when excess metal is present (*8*). In this study, we sought to exhaustively evaluate the effects of amino acid substitutions in metal binding ligands. We did not typically consider mutants requiring an excess of metal because such proteins would be unlikely to be stable under physiological conditions. Consistent with the findings of Christianson and co-workers, we also identified H101N or -D and H126N or -Q mutations in conjunction with second-shell changes. We found that no first-shell ligand substitution resulted in significant activity (Tables S1 and S2 of the Supporting Information). Second-shell residues D181 and S230 alone or in combination showed the greatest tolerance to amino acid substitutions, with the solvent-exposed D181 position accepting nearly all amino acids. Second-shell residue S230 is buried in the interior of the protein, and predictably, its substitution with only small- to medium-sized residues resulted in active enzymes.

Although we identified a large number of dual substitutions at D181 and S230, none of these had a k_{cat}/K_M greater than that of the wt enzyme. However, we found two single second-shell substitutions, S230G and S230C, that conferred a significant increase in k_{cat}/K_M compared to that of the wt enzyme (2600 ± 420 and 2180 ± 360 s^{-1} mM^{-1}, respectively, compared to 1260 ± 330 s^{-1} mM^{-1} for wt). The 2-fold increase in the k_{cat}/K_M of Co-hArgI-S230G is primarily described by a significantly lower K_M. A lower K_M is also observed with Mn^{2+} substitution, revealing that these effects are independent of the nature of the catalytic metal. The S230G variant substituted with either Mn^{2+} or Co^{2+} also exhibited a reduced product inhibition constant indicating enhanced coordination of the ligand. S230 is the second-shell ligand to H101 that coordinates metal A (M_A), suggesting that with the S230G mutation, M_A is in a more favorable environment for coordinating substrate and product ligands. The ascending limb pK_a value of the pH dependence of k_{cat}/K_M in the S230G variant was depressed from 7.5 for wt Co-hArgI to 7.0 ± 0.1, consistent with the notion that this variant has an increased capacity for stabilizing ligands of water/hydroxide or substrate or product.

It has been proposed that the effect of first- and second-shell mutations in metallohydrolases can be explained on the basis of the stabilization and/or destabilization of a negatively charged nucleophilic hydroxide molecule for attack on the substrate (*14*, *15*). Consistent with this model, the S230G mutation appears to stabilize bound ligands such as water/hydroxide. In comparison to the wt enzyme, the variant S230C constitutes a single atom substitution of oxygen with sulfur. This variant has a K_M value within error of that of wt but a higher k_{cat}. This single-atom change further resulted in an altered pH dependence of k_{cat}/K_M, displaying a narrow bell-shaped curve with an increased ascending limb pK_a of 7.8 ± 0.1 and a decreased descending limb pK_a value of 9.0 ± 0.1. As seen from the decreased relative activity of variants that incorporate a negative charge at position S230 (S230D value ~74% of wt k_{cat}/K_M), it is likely that the altered pH rate dependence of S230C reflects in part the ionization of the introduced thiol side chain, which under alkaline conditions would introduce a negatively charged thiolate ion and thus destabilize coordination of the nucleophilic hydroxide molecule.

The second-shell ligands in metalloenzymes are thought to stabilize the electrostatic environment between the metal and ligands and to orient the inner ligands for optimal coordination. Noteworthy is the finding that the S230A or S230G mutation occurred in nearly 50% of the variants identified from library 5 (Table S4 of the Supporting Information). It is possible that the S230G (or S230A) variant contains a water molecule that now acts as a hydrogen bond acceptor for H101, but perhaps H101 is reoriented in position, allowing M_A to more easily coordinate ligands (we are working on confirming or denying this hypothesis through structural analysis). The lower K_M and K_I values observed with the S230G mutation containing either Mn^{2+} or Co^{2+} cations suggest that M_A is now a stronger Lewis acid. Earlier, we proposed that the dinuclear metal center of arginase, especially with Co^{2+}, may play a role in ionizing and coordinating an imino guanidine nitrogen of substrate L-Arg (*6*). We suspect that although Mn^{2+} has less intrinsic affinity for N ligands, it can also directly coordinate a substrate guanidine nitrogen during catalysis, an effect enhanced by contributions from the second-shell metal ligands. The pH dependence of k_{cat} of Mn^{2+}-hArgI-D181N/S230G has a single ascending pK_a depressed by 0.4 pH unit compared to that of the wt enzyme [in contrast, ionizations in the free enzyme and free substrate (k_{cat}/K_M) are within error of that of wt]. These changes in the second shell reflect an ionization important to the Michaelis complex (ES), suggestive of deprotonation of the substrate guanidinium and coordination of the neutral guanidine. The structure of arginase from *Bacillus caldovelox* (Protein Data Bank entry 3CEV) shows a single Mn^{2+} in the M_A site coordinating a substrate L-Arg molecule by a terminal amino nitrogen (*16*). Similarly, a recent human arginase structure (Protein Data Bank entry 3MFV) in a complex with the inhibitor 2-aminohomohistidine, which is isosteric to L-Arg, shows an imidazole N atom coordinated to M_A (note that M_B is present in this structure) (*17*). Also, the structure of rat arginase I bound to the L-Arg analogue 2(*S*)-amino-6-boronohexanoic acid (Protein Data Bank entry 1D3V) is consistent with coordination of a tetrahedral intermediate through M_A (*18*). This structural information taken together with the observed changes in ligand binding when the S230 second-shell ligand to M_A is altered strongly suggests that substrate L-Arg is coordinated to M_A during the reaction and that the Lewis acidity of M_A is modulated by the second-shell ligand to H101.

CONCLUSION

The first-shell metal ligands of arginase are strictly conserved across all known species and are essential to proper binding and coordination of the dinuclear metal center. The second-shell metal ligands are also highly conserved across most species, although the ligands to H101, D124, and H126 are not absolutely essential. Experimentally observing such a surprising amount of second-shell plasticity in comparison with phylogenetic analysis suggests that kinetic optimization was not the only driving force for arginase in the course of evolution. Mechanistically, the second-shell ligand hydrogen bonded to H101 that is coordinating M_A of the active site appears to have a significant role in modulating the Lewis acidity in coordinating ligands essential to the arginase-catalyzed reaction. Furthermore, the variants identified with enhanced catalytic activity may be of therapeutic interest for the treatment of L-Arg auxotrophic cancers.

SUPPORTING INFORMATION AVAILABLE

One experimental procedure paragraph detailing library construction, one figure of the relative pH dependence of two variants, and four tables detailing the relative activity of isolated library variants. This material is available free of charge via the Internet at http://pubs.acs.org.

REFERENCES

1. Cama, E., Emig, F. A., Ash, D. E., and Christianson, D. W. (2003) Structural and functional importance of first-shell metal ligands in the binuclear manganese cluster of arginase I. *Biochemistry 42*, 7748–7758.
2. Dowling, D. P., Costanzo, L. D., Gennadios, H. A., and Christianson, D. W. (2008) Evolution of the arginase fold and functional diversity. *Cell. Mol. Life Sci. 65*, 2039–2055.
3. Christianson, D. W., and Cox, J. D. (1999) Catalysis by metal-activated hydroxide in zinc and manganese metalloenzymes. *Annu. Rev. Biochem. 68*, 33–57.
4. Viator, R. J., Rest, R. F., Hildebrandt, E., and McGee, D. J. (2008) Characterization of *Bacillus anthracis* arginase: Effects of pH, temperature, and cell viability on metal preference. *BMC Biochem. 9*, 15.
5. McGee, D. J., Zabaleta, J., Viator, R. J., Testerman, T. L., Ochoa, A. C., and Mendz, G. L. (2004) Purification and characterization of *Helicobacter pylori* arginase, RocF: Unique features among the arginase superfamily. *Eur. J. Biochem. 271*, 1952–1962.
6. Stone, E., Glazer, E. S., Chantranupong, L., Cherukuri, P., Breece, R. M., Tierney, D. L., Curley, S. A., Iverson, B. L., and Georgiou, G.

(2010) Replacing Mn^{2+} with Co^{2+} in Human Arginase I Enhances Cytotoxicity Towards L-Arginine Auxotrophic Cancer Cell Lines. *ACS Chem. Biol. 5*, 333–342.
7. Scolnick, L. R., Kanyo, Z. F., Cavalli, R. C., Ash, D. E., and Christianson, D. W. (1997) Altering the binuclear manganese cluster of arginase diminishes thermostability and catalytic function. *Biochemistry 36*, 10558–10565.
8. Cavalli, R. C., Burke, C. J., Kawamoto, S., Soprano, D. R., and Ash, D. E. (1994) Mutagenesis of rat liver arginase expressed in *Escherichia coli*: Role of conserved histidines. *Biochemistry 33*, 10652–10657.
9. Orellana, M. S., López, V., Uribe, E., Fuentes, M., Salas, M., and Carvajal, N. (2002) Insights into the interaction of human liver arginase with tightly and weakly bound manganese ions by chemical modification and site-directed mutagenesis studies. *Arch. Biochem. Biophys. 403*, 155–159.
10. Knipp, M., and Vasak, M. (2000) A colorimetric 96-well microtiter plate assay for the determination of enzymatically formed citrulline. *Anal. Biochem. 286*, 257–264.
11. Segel, I. H. (1975) Enzyme kinetics: Behavior and analysis of rapid equilibrium and steady state enzyme systems, Wiley, New York.
12. Kiefer, L. L., Paterno, S. A., and Fierke, C. A. (1995) Hydrogen bond network in the metal binding site of carbonic anhydrase enhances zinc affinity and catalytic efficiency. *J. Am. Chem. Soc. 117*, 6831–6837.
13. Perozich, J., Hempel, J., and Morris, S. M., Jr. (1998) Roles of conserved residues in the arginase family. *Biochim. Biophys. Acta 1382*, 23–37.
14. Christianson, D. W., and Fierke, C. A. (1996) Carbonic anhydrase: Evolution of the zinc binding site by nature and by design. *Acc. Chem. Res. 29*, 331–339.
15. Krebs, J. F., Ippolito, J. A., Christianson, D. W., and Fierke, C. A. (1993) Structural and functional importance of a conserved hydrogen bond network in human carbonic anhydrase II. *J. Biol. Chem. 268*, 27458.
16. Bewley, M. C., Jeffrey, P. D., Patchett, M. L., Kanyo, Z. F., and Baker, E. N. (1999) Crystal structures of *Bacillus caldovelox* arginase in complex with substrate and inhibitors reveal new insights into activation, inhibition and catalysis in the arginase superfamily. *Structure 7*, 435–448.
17. Ilies, M., Di Costanzo, L., North, M. L., Scott, J. A., and Christianson, D. W. (2010) 2-Aminoimidazole Amino Acids as Inhibitors of the Binuclear Manganese Metalloenzyme Human Arginase I. *J. Med. Chem. 53*, 4266–4276.
18. Cox, J. D., Kim, N. N., Traish, A. M., and Christianson, D. W. (1999) Arginase−boronic acid complex highlights a physiological role in erectile function. *Nat. Struct. Mol. Biol. 6*, 1043–1047.